Hindawi
Advances in Materials Science and Engineering
Volume 2022, Article ID 5625427, 8 pages
https://doi.org/10.1155/2022/5625427

Research Article

Post-Surface Processing and Virtual Simulation Analysis of Ball-Punch Test on CP-Ti Material

Ananda Mohan Vemula,[1] **G. Chandra Mohan Reddy**,[2] **M. Manzoor Hussain**,[3] **Atul Kumar**,[4] **Naresh Kumar**,[5] **and Haiter Lenin Allasi**[6]

[1]*Department of Mechanical Engineering, Guru Nanak Institutions Technical Campus, Hyderabad, Telangana, India*
[2]*Department of Mechanical Engineering, Chaitanya Bharathi Institute of Technology, Hyderabad, Telangana, India*
[3]*Department of Mechanical Engineering, Jawaharlal Nehru Technological University, Hyderabad, Telangana, India*
[4]*SET, Mody University of Science and Technology, Laxmangarh-332311, Sikar, Rajasthan, India*
[5]*Department of Mechanical Engineering, Manda Institute of Technology, Raisar, Bikaner, Rajasthan, India*
[6]*Department of Mechanical Engineering, WOLLO University, Kombolcha Institute of Technology, Post Box No: 208, Kombolcha, Ethiopia*

Correspondence should be addressed to Ananda Mohan Vemula; happymohan@yahoo.com and Haiter Lenin Allasi; drahlenin@kiot.edu.et

Received 11 November 2021; Accepted 20 February 2022; Published 11 March 2022

Academic Editor: J.T. Winowlin Jappes

The titanium alloy is one of the prime materials for many engineering applications. It has been recommended for the components in automotive engines, power sector, biomedical industries, and more applications. It is due to the unique properties of the material with good strength and corrosion resistance. However, it is very challenging to handle Ti-based materials in manufacturing sectors without damaging the metallurgical quality. Thus, an attempt made to study the deformability of the CP-Ti material through ball–punch test to represent the stress, strain, and formability limit during mechanical loading and plastic deformation. The experiments are conducted following the ASTM E643 standards to study the material behavior. The maximum cupping reached to a height of 8.69 mm and got teared at the peak of doom. The separation has induced grain detachment due to tensile loading. The same condition is used to simulate with PAM STAMP™ software and 8.48 mm is the maximum cupping height achieved. The different is 0.21 mm. The results are interesting with similar observations and found acceptable to study the deformation.

1. Introduction

In the last two decades, demand for titanium alloy and its research are found increased in automobile components, biomedical engineering, and food processing industries [1–3]. These alloys are recommended for structural engineering and load bearing systems and widely used as alternate materials for biomedical components. The titanium alloy offers best performance in automobile components subjected to extreme load/suspension systems. Especially, the structure component should have high corrosion resistance, good formality, and high strength with low modulus to sustain reliable service period of the structure developed [4]. Literature is available to discuss about the processing of titanium alloys [5]. In general, the titanium alloys are widely used in aero jet engine components to make compressor disc, fan doom, and fan blades. It should possess high strength with less weight, less fatigue, and creep failures [6]. Jiang and Huang investigated and reported the grain replacement and effects on mechanical forming of Ti alloy. While processing the material through mechanical loading, the crystalline structure of alloy varies with respect to process condition. The commercial pure titanium (CP Ti) is HCP (hexagonal closely packed) structure below 800°C and

BCC (body centered cubic) above 800°C temperatures [7]. The CP Ti exhibits low elastic modulus limited plastic sag while deformation. While working with CP-Ti alloy, the deformed structure reveals with twinning effect due to the strength differential ratio with respect to direction of forming [8]. However, the studies on deformability and its process are yet to explore for titanium alloy. It has been reported that the plastic deformation of titanium and its alloys at room are found difficult [9]. The Ti and Ti-based alloys are induced to produce work hardening (rapidly) and strain leads to failure while cold working (mechanical loading and deformation at room temperature) [9, 10]. Since, there is a need for detailed studies deformation and its formability during mechanical processing.

In this study, the research has been focused on mechanical loading, plastic deformability, and structural analysis of the commercially pure titanium (CP-Ti) alloy. The ball-punch deformation test was performed on Cp-Ti alloy to forecast the formability limits and its strain during deep drawing. From the analysis the Erickson number, peak load, deformability, FLD, and its strain are calculated [11, 12]. In order to reduce the materials wastage, process time, and cost factor, the experimentations are performed through virtual systems, and the optimal results are verified through real-time instruments. The PAM STAMP™ is the commercially available simulation package used to study the deformation of engineering materials [13, 14]. The formability and deformability pressure of the material are the main components of the cupping test. The validation of the results from ball-punch analysis and FE simulation are inspiring in recent research situations [15, 16]. The highlight the research state of art is that there is no study to report on mechanical deformation of Ti alloys through ball-punch deformation test and simulated with PAM STAMP™ software. Therefore, an attempt is made to study the deformability of commercially pure titanium alloy through ball-punch deformation test and simulated with PAM STAMP™ software.

2. Materials and Method

The commercially pure titanium (Cp-Ti) alloy is chosen as a test material. The nomination composition and the physical dimension of the test sample are given in Table 1. The samples are cleaned with acetone to degrease and ensured the samples are ready to investigate. Investigations are performed in ball-punch (Erichsen Cupping) test (Sheet and Strip Metal Testing Machine Model 111) following standard procedure of ASTM E643 (equivalent to ISO 20482). The deformability of CP-Ti alloy is studied using ball-punch tester and the same was simulated with PAM STAMP™ simulation software. The pictorial representation of ball-punch test and proposed research plan is shown in Figure 1. The mechanical test parameters and the specifications for ball-punch instrument are given in Table 2. Figure 2 shows the detail sketch of ball-punch die arrangements following ASTM standards.

The estimation of forming limit diagram depends on the axial strain caused in major axis and minor axis. In addition, the dimension of the cup used for deformation is considered as a factor. It is also based on the tensile test results generated by testing the dog bone-shaped specimen and the details are given in Table 3. The fundamental sketch of FLD with different zones is shown in Figure 3.

Table 1: The nomination composition of Cp-Ti alloy and the physical dimension.

Input factors	Range
Thickness	1.20 mm
Size of sheet	90 mm × 90 mm ($l \times b$)
Density	4.51 g/cc
Brinell's hardness	120 BHN

Equation (1) represents the mathematical relation which is used to study the yield/fracture point of the material under cupping process [17]:

$$F|\sigma_2 - \sigma_3|a + G|\sigma_3 - \sigma_1|a + H|\sigma_1 - \sigma_2|a = 1. \quad (1)$$

It is assumed to be an anisotropy material having standard constants. On substitution of standard details, the relative equation is further given in

$$R_0|\sigma_2 - \sigma_3|a + R_{90}|\sigma_3 - \sigma_1|a + R_{90}R_0|\sigma_1 - \sigma_2|a = R_{90}(1 + R_0)Xa,$$
$$\sigma = K \cdot \left(\varepsilon_0 + \varepsilon_p\right)^n. \quad (2)$$

The above equations are related to Krupkowsky law. It is directly related to the stain components and its coefficient.

The mechanical boundary conditions for PAM STAMP TM are obtained by fixing the blank holder and die is fixed (all degrees of freedom); then, punch is allowed to indent on the CP-Ti sheet in Z direction till the crack appears.

3. Results and Discussion

The deformability of CP-Ti alloy is performed as per the ASTM standards and the results are discussed with reference to macroscopic (visual) analysis, microscopic analysis, simulated analysis, and FLD plots. The photo image of the mechanical deformed CP-Ti sample is shown in Figure 4. At the top of doom, the material deformed during cupping found stretched and the thickness got reduced. That is, the action of the metal atoms induced due to tensile loading and separation occurs. It is an action of sliding of metal atoms with respect to the mechanical force and so called as slipping. On continuous loading, the slipping persuades the metal thinning to cracking and the element cracking occurs. For better illustration, the traction-separation of the metal is illustrated in Figure 5. It is physically visible that the fracture is in the form of typical linear traction-separation response. The crack growth is analyzed over the fractured samples, and it is under two conditions. The crack is initiated in the perpendicular direction of the punch, and it depends on specimen thickness and maximum principal stress criterion. During continuous loading (in tensile loading), the continuous separation was noticed along the crack surface. When the stiffness (δ) of the material is greater than the crack stiffness (δ_o), the traction occurs. The traction is a

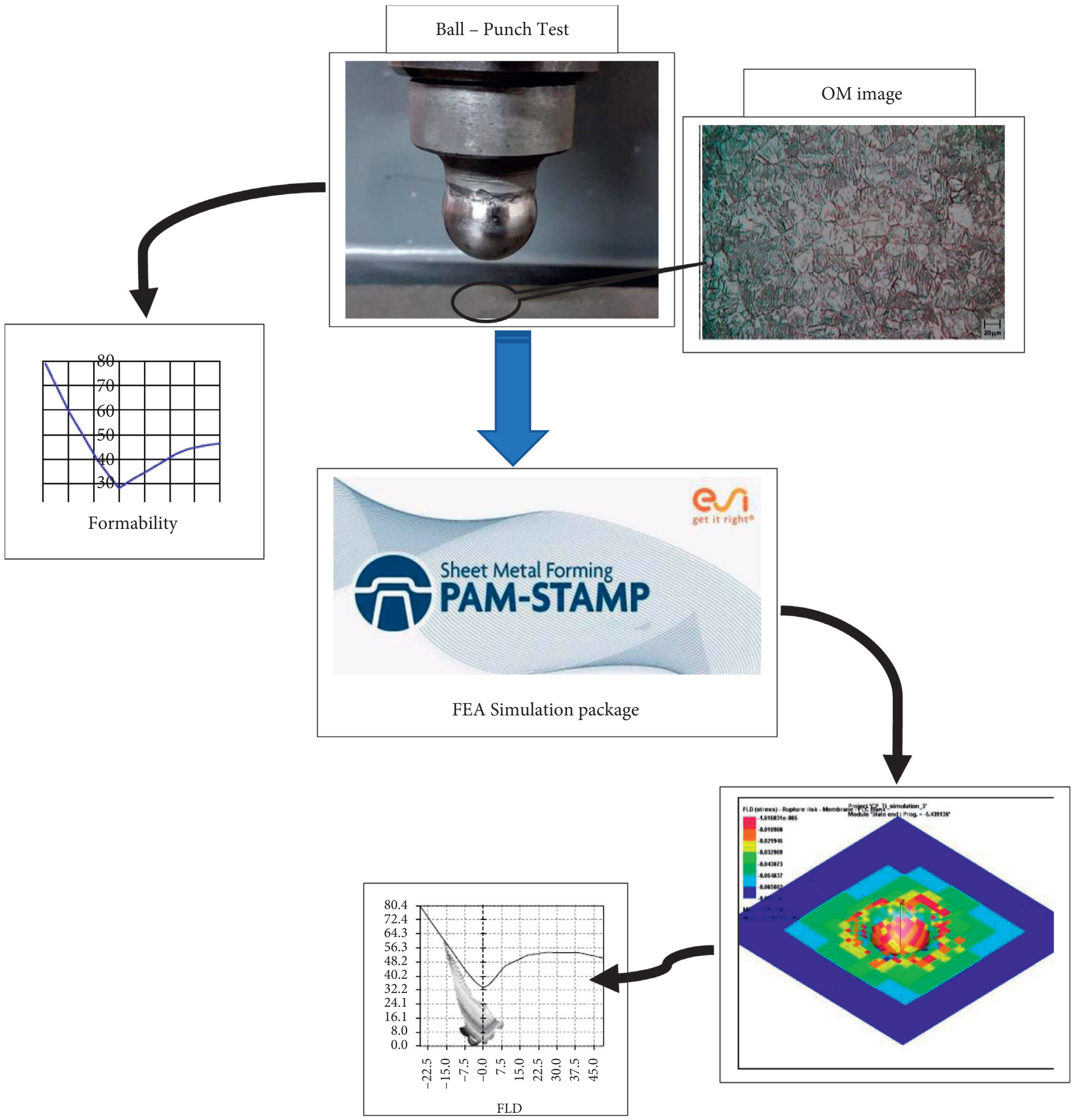

Figure 1: Work plan of the CP-Ti alloy formability study.

Table 2: The standard parameters and specifications for the ball-punch tester.

Sl. no.	Description	Value
1	Stroke of punch	5 mm/min to 20 mm/min
2	Diameter of the punch ($d1$)	20 mm
3	Inside corner radius of die ($R2$)	0.75 mm
4	Outside corner radius of die ($R1$)	0.75 mm

plastic deformation of a material in all coordinate (multi-direction) induced due to mechanical force. It has been reported that the doom fracture and the crack propagation depend on the materials properties [18].

Furthermore, the microstructural analysis is carried out on the fractured samples. The microstructure of the CP-Ti material before and after mechanical loading is recorded under a high-end metallurgical microscope and displayed in Figure 6. It is clear that the CP-Ti material used for the mechanical loading (ball-punch deformation test) is having an austenitic structure. At the same, on mechanical loading, the CP-Ti material has been deformed and the crack is initiated. The microstructure observed near to the separation (crack) is identified with the deformed grain structure. It has

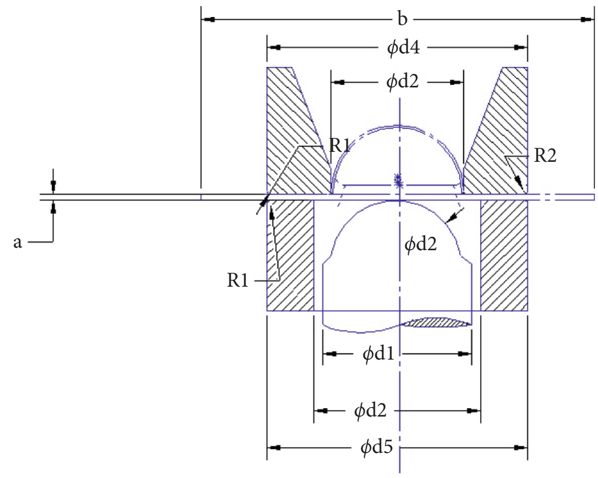

Figure 2: Schematic representation of ball-punch (Erichsen cupping) test methodology.

Table 3: Physical and mechanical properties of CP-Ti material.

Properties	Range	Units
Yield load	kN	3.2
Max. load	kN	4
Yield stress	MPa	269
U.T.S	MPa	336
% of elongation	%	52.28
Poisson's ratio	—	0.37
Modulus of elasticity	GPa	105
Coefficient of linear expansion		8.4×10^{-6}/K

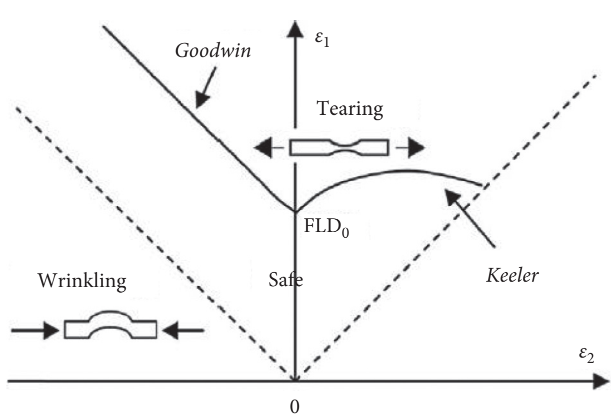

Figure 3: Fundamental representation sketch of forming limit diagram representing strains and different regimes.

also caused mechanical detachment between the grain traction. The rate of crack depends up on the ball-punch load coatings and the material thickness. During the loading, the material inclined to mechanical strain and further loading will induce the material to cracking. This is called tearing due to tension load and the deformed material with different regimes.

In continuation to metallurgical and mechanical observations on CP-Ti deformation, finite element analysis is carried out. To study the stress and strain rate on deformed material, the deformability diagram predicted through PAM STAMP™ numerical analysis software is used. With the same load condition, the material is simulated for stress and strain induced on ball-punch (cupping) test. The deformability of the material will indicate the major issues such as wrinkle, stretching, surface waviness, and insufficient formability from the analysis. Figure 7 illustrates the FLD graph plotted for strain developed from the simulation results and to locate points on different regimes for better understanding. The deformability rate of the material is recorded from the analysis and it is reported with respect to the axis coordinates. The results are as minor strain on abscissa (x-coordinate) and major strain on vertical axis (y-coordinate). From the cupping test, the fracture zone is indicated with dark spots over the deformed zone. The variations in the deformability is indicated with different color marks. The deformation of the material is as visualized in the photo image (Figures 4 and 5). Figure 8 shows the simulated ball-punch deformed area and strain distributed zone. It is clear to confirm that the center of the circular area has maximum strain and the rate recorded in the FLD diagram. Inset shows the maximum cupping height produced in the simulation. While comparing the results with standard FLD boundaries, the CP-Ti material is prone to some strain points above the Keeler line indicating material failure due to tearing. There are no spots around the Wrinkling or Good line regions. The test material has a major spot between the safe and Keeler line indicating the subregions are under safe

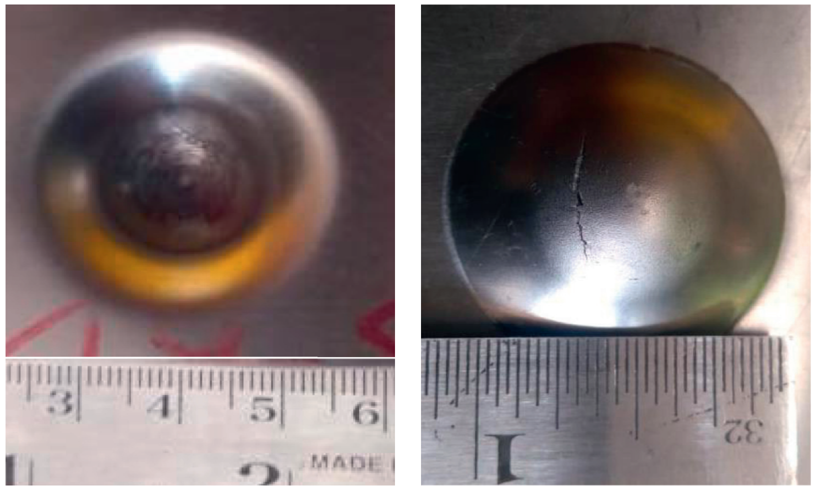

(a) (b)

Figure 4: Photo image of the CP-Ti material after ball-punch mechanical deformation. (a) Back view. (b) Front view.

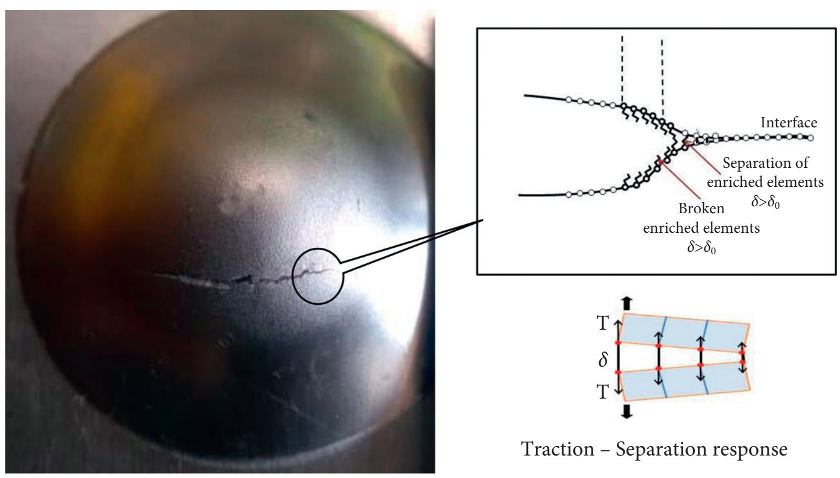

Figure 5: CP-Ti material to illustrate the traction-separation during mechanical loading.

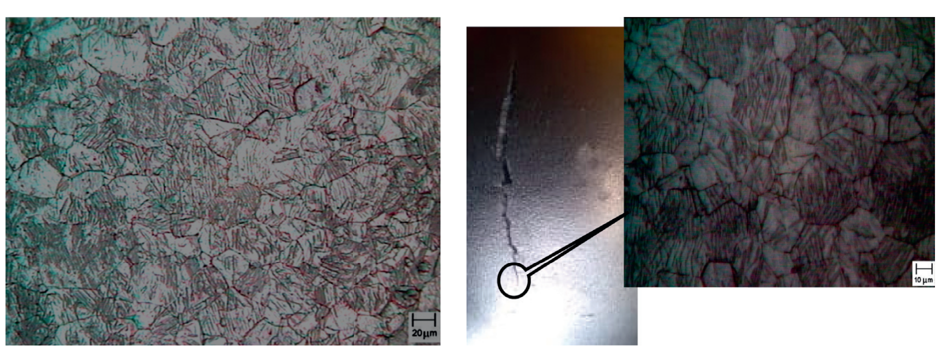

(a) (b)

Figure 6: Microstructural changes in CP-Ti sample before and after deformation. (a) Original microstructure. (b) Deformed microstructure.

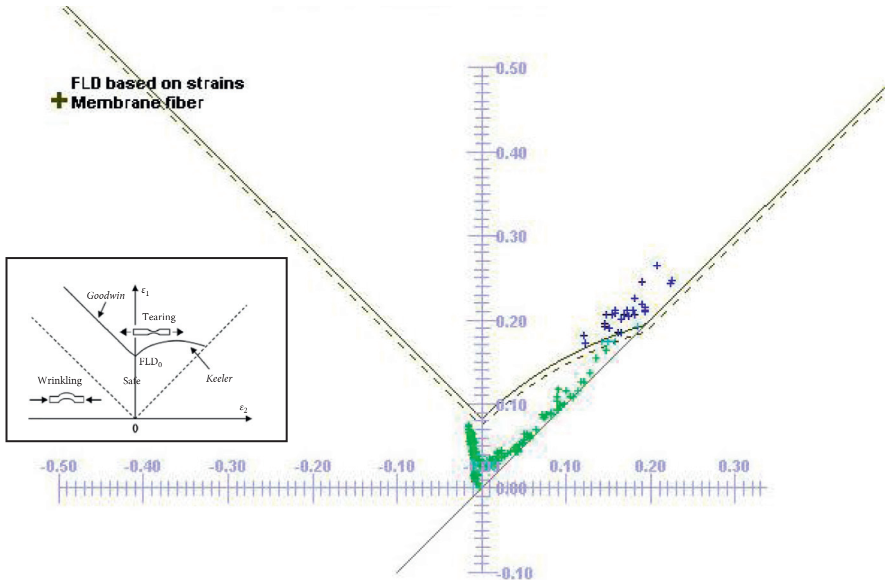

Figure 7: Graph to represent the strain developed on CP-Ti material induced while testing through formability limit diagram (FLD).

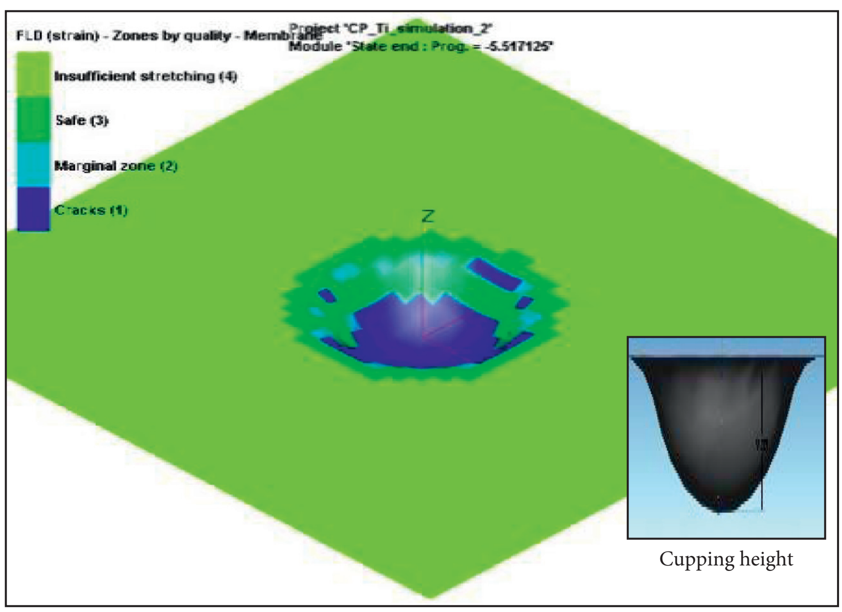

Figure 8: Simulated results indicating the FLD strain zones recorded after ball-punch test.

conditions. As a result, the numerical analysis of the material deformed and the tearing revealed to be similar with the experimental data.

Inference made on strain development: the simulation is also carried out to study the stress development during the same process. Figure 9 shows the FLD diagram with stress concentration of CP-Ti material during the ball-punch test. The spots are identified very close to Keeler line indicating the stress developed while material failure. During punching, the strain found more and continued to surface tear at the top of doom. At the same region, the FLD diagram indicates that the stress has been aggregated over the Keeler line with dense spots. Figure 10 shows the stress distribution on deformed area of ball-punch test sample results achieved through PAM STAMP™ simulation software. Red color indicates the maximum stress induced at the top of cup doom and found reducing in adjunct area of the sample with different colors of representation. As discussed above, the traction cum separation during tensile shear observed on the test sample is confirmed with the simulated results. From the experimental analysis and simulation method, the cupping height of the deformed material is measured for comparison. Three sets of experiments were done under the same test condition and simulation was carried out thrice for repeatability. The average results obtained for the analysis is tabulated in Table 4. The average cupping height of the deformed materials from the experiments and simulation are as 8.69 mm and 8.48 mm, respectively. The difference in

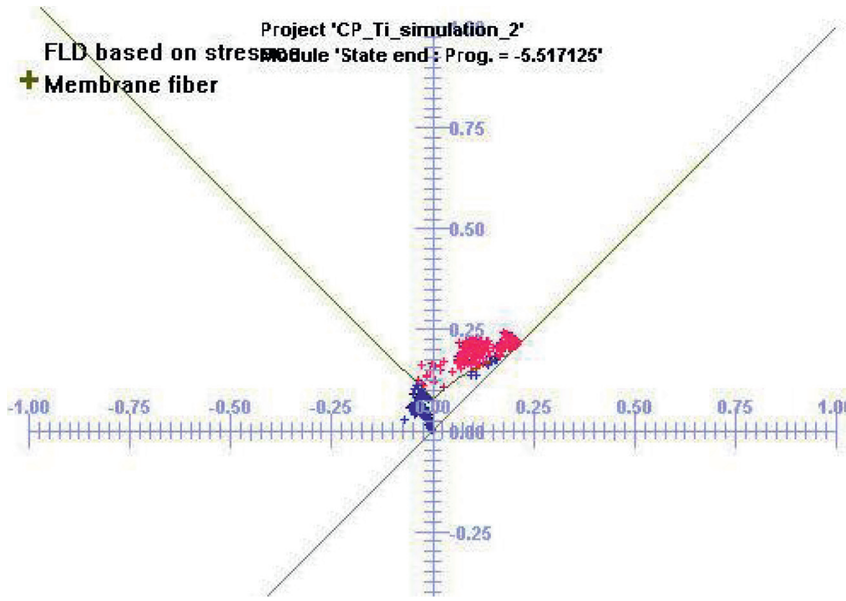

Figure 9: Graph to represent the stress developed on CP-Ti material induced while testing through formability limit diagram (FLD).

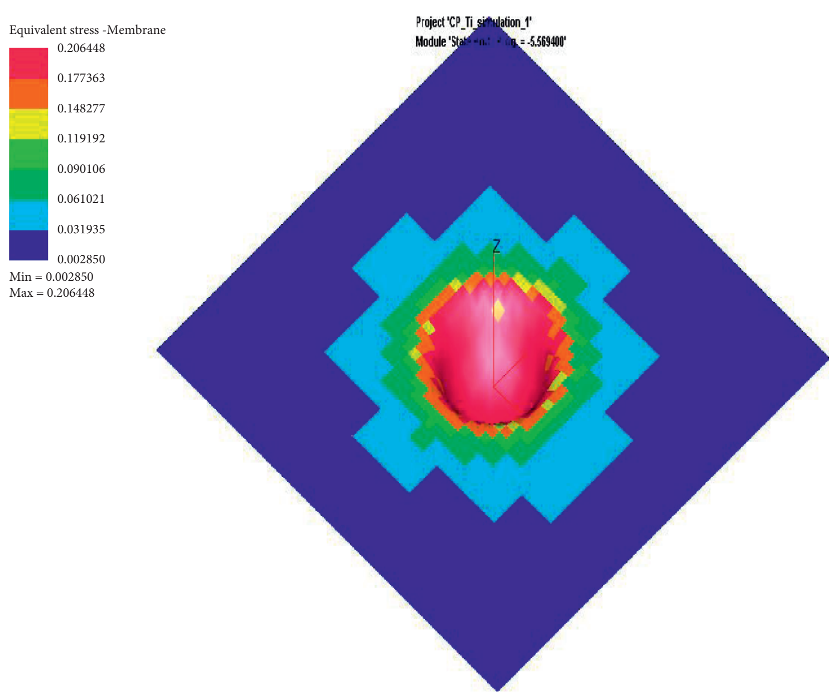

Figure 10: Simulated results indicating the stress distribution over the FLD zones recorded after the ball-punch test.

Table 4: Cupping test results from experiments and simulation.

Materials	Ball-punch test	Exp value (mm)	Sim value (mm)	Difference (mm)
CP-Ti	Cup height	8.69	8.48	0.21

cup height for experiments and simulation is 0.21 mm. It specifies that the formability value is similar in both the tests. Therefore, the same procedure can be used to study the deformation of the CP-Ti material with variation sections and materials composition.

4. Conclusions

The research presents the experimental investigation through the ASTM E643 ball-punch deformation test on CP-Ti material. Furthermore, for investigation, the results are compared with simulation of the same experiments performed in PAM STAMP^{TM} simulation software. It has been confirmed that the CP-Ti alloy is perfect to deform under mechanical loading. During loading, the maximum height of the cupping found 8.69 mm in physical setups and surface fracture at the top of doom. The difference in cup height for experiments and simulation is 0.21 mm. The fracture is noticed perpendicular to ball-punch axis creating tensile load. The continuous tensile load has induced the grains to detach from each other and cause the adjunct layer to become vulnerable. The rate of stress and strain developed during deformation was found to be aggregated over the top of doom. The same has been confirmed from the simulation package, and FLD diagram has been drawn. The results achieved from mechanical and virtual analysis are similar to compare. Therefore, the proposed technique can support to study the behavior of the material using ball-punch deformation for different sections and is quite informative to report the quality of the material. [19].

Data Availability

No data were used to support the findings of the study.

Conflicts of Interest

The authors declare that they have no conflicts of interest.

Acknowledgments

The authors thank the MIDHANI management for providing commercially pure titanium (CP-Ti) material for this research work.

References

[1] M. Yamada, "An overview on the development of titanium alloys for non-aerospace application in Japan," *Materials Science and Engineering*, vol. 213, no. 1-2, pp. 8–15, 1996.

[2] M. J. Jackson and W. Ahmed, "Titanium and Titanium Alloy Applications in Medicine," *Surface Engineered Surgical Tools and Medical Devices*, pp. 533–576, Springer, Boston, MA, 2007.

[3] R. Hariharan, R. Raja, R. J. Golden Renjith Nimal, M. R. A. Refaai, S. Ravi, and L. A Haiter, "Characterization of TiZrN and TaZrN nano composite multilayer coating deposited via RF/DC magnetron sputtering on AISI4140 steel," *Advances in Materials Science and Engineering*, vol. 2021, Article ID 8273708, 10 pages, 2021.

[4] L.-C. Zhang and L.-Yu Chen, "A review on biomedical titanium alloys: recent progress and prospect," *Advanced Engineering Materials*, vol. 21, no. 1- 29, Article ID 1801215, 2019.

[5] A. K. Sachdev, K. Kulkarni, Z. Z. Fang, R. Yang, and V. Girshov, "Titanium for automotive applications: challenges and opportunities in materials and processing," *Journal of Occupational Medicine*, vol. 64, no. 5, pp. 553–565, 2012.

[6] M. Manish Kumar, S. Prakash Rao, and S. P. Jani, "Design and analysis of aero fin blades utilized in cargo aero plane," *Materials Today Proceedings*, vol. 45, pp. 1939–1944, 2021.

[7] C.-P. Jiang and Z. H. Huang, "Finite element modeling of grain size effect on the mechanical properties and deformability of titanium alloy in equal channel angular pressure," *Key Engineering Materials*, vol. 661, pp. 91–97, 2015.

[8] "Prediction of forming limit curve for pure titanium sheet," *Transactions of Nonferrous Metals Society of China*, vol. 28, no. 2, pp. 319–327, 2018.

[9] U. K. Ugurchiev and V. V. Stolyarov, "Deformability and microhardness of large-grain titanium alloys in rolling with pulsed current," *Journal of Machinery Manufacture and Reliability*, vol. 41, no. 5, pp. 404–406, 2012.

[10] L. Zhu, Y. D. Song, and J. Chen, "Modeling of multi-scale fatigue crack growth in titanium alloy TC4," *Iran J Sci Technol Trans Mech Eng*, vol. 45, 2020.

[11] R. Udaykumar, G. C. Reddy, and R Chandramohan, "Evaluation of erichsan number and peak load of sheet metals," *International Journal of Advanced Materials Manufacturing and Characterization*, vol. 3, no. 1, pp. 381–383, 2013.

[12] M. Singh, A. K. Choubey, and C. Sasikumar, "Formability analysis of aluminium alloy by erichsen cupping test method," *Materials Today Proceedings*, vol. 4, no. 2, pp. 805–810, 2017.

[13] M. A. Ablat and A. Qattawi, "Numerical simulation of sheet metal forming: a review," *International Journal of Advanced Manufacturing Technology*, vol. 89, no. 1-4, pp. 1235–1250, 2017.

[14] A. Wang, O. El Fakir, J. Liu et al., "Multi-objective finite element simulations of a sheet metal-forming process via a cloud-based platform," *International Journal of Advanced Manufacturing Technology*, vol. 100, no. 9-12, pp. 2753–2765, 2019.

[15] C. Schwindt, F. Schlosser, M. A. Bertinetti, M. Stout, and J. W. Signorelli, "Experimental and Visco-Plastic Self Consistent evaluation of forming limit diagrams for anisotropic sheet metals: an efficient and robust implementation of the M-K model," *International Journal of Plasticity xxx*, vol. 73, 2015.

[16] X. Ma, F. Li, J. Li, Q. Wang, Z. Yuan, and Y. Fang, "Analysis of forming limits based on a new ductile damage criterion in St14 steel sheets," *Materials and Design*, vol. 68, pp. 134–145, 2014.

[17] T. Altan and A. E. Tekkaya, *Sheet Metal Forming Fundamentals*, ASM International, Geauga, 2012.

[18] J. M. Sim and Y. S. Chang, "Crack growth evaluation by XFEM for nuclear pipes considering thermal aging embrittlement effect," *Fatigue and Fracture of Engineering Materials and Structures*, vol. 42, pp. 1–17, 2018.